

International Conference on Space Optics—ICSO 2018

Chania, Greece

9–12 October 2018

Edited by Zoran Sodnik, Nikos Karafolas, and Bruno Cugny



Post-processing correction of stray-light in space instruments: application to the 3MI earth observation instrument

L. Clermont

C. Michel

E. Mazy

Y. Stockman



Post-processing correction of stray-light in space instruments: application to the 3MI Earth observation instrument

L. Clermont*^a, C. Michel^a, E. Mazy^a, Y. Stockman^a

^aCentre Spatial de Liège, STAR Institute (Space Sciences, Technologies and Astrophysics Research), Avenue du Pré-Aily, 4031 Angleur, Belgium

ABSTRACT

Stray-light is a major concern in optical instruments and in particular for space missions. While many methods exist to reduce the stray-light by means of hardware optimization, manufacturing capabilities set the limit of the stray-light rejection that can be achieved. Hence, there are situations where the scientists that use the data require stray-light level lower than what hardware alone can reach. This is for example the case of the Metop-SG 3MI mission, which despite a well optimize instrument doesn't reach as is the performance requirement. In such situations, it is necessary to add in the processing chain of the data a stray-light correction algorithm which further reduces the stray-light level. This paper discusses the algorithm implemented for 3MI.

Keywords: Stray-light correction, post-processing, space optics, Earth observation, correction algorithm

1. INTRODUCTION

Stray-light is undoubtedly a concern of great importance for Earth observation instruments, and generally speaking of optical instruments. Defined as unwanted light reaching the detector [1], the effect of stray-light is the broadening of the point spread function as well as the apparition on the image of unwanted features. As a consequence, the image quality is decreased and so is the added value scientists can extract from the observation data. Stray-light can arise due to multiple optical phenomena in the instrument, for example multiple reflections in the lenses, or scattering on the optics or even on the mechanics. Many methods exist to reduce the level of stray-light as far as it concerns hardware [1]: optimizing the optical setup, applying anti-reflections coatings on the lenses, using baffles to block unwanted paths and using black coatings to reduce the scattering on the non-optical surfaces. The capabilities of hardware as a mean to reducing stray-light is however limited [2]. No black coating perfectly absorbs light, no anti reflection completely avoids ghost reflections and optical surfaces always have some roughness and are subject to contaminations. Hence, in the most constraining applications, it is not always possible to design and manufacture an instrument which presents sufficiently low stray-light levels. This was for example the case of the METOP-SG 3MI instrument, consisting of two multispectral instruments operating in the VNIR and SWIR spectral ranges [3]. For that reason, a stray-light correction algorithm was developed to reduce the stray-light by about 2 orders of magnitude compared to the initial level [2]. More specifically, the performance requirement is that for an extended scene with half the FOV illuminated at L_{max} and the other half at $L_{ref}=L_{max}/10$, the corrected signal should present a residual stray-light error below 0.17% of the L_{ref} signal (equation 1). Figure 1-left shows the nominal (stray-light free) signal at detector for such an extended scene, while the Figure 1-right shows the associated stray-light. Consequently, it is required to be able to estimate that stray-light profile with an accuracy given by equation 1. The algorithm developed for 3MI works based on the calibration of the stray-light patterns as a function of the field of view, called the Spatial Point Source Transmittance map (SPST). As only a limited number of fields can be calibrated, methods were developed to interpolate the SPST maps for intermediary fields. In this paper, we describe with more details the effect of the binning and the SPST maps interpolation method.

$$\frac{|I_S - I_{corr}|}{I(L_{ref})} \leq 0.17\% \quad (1)$$

*lionel.clermont@uliege.be

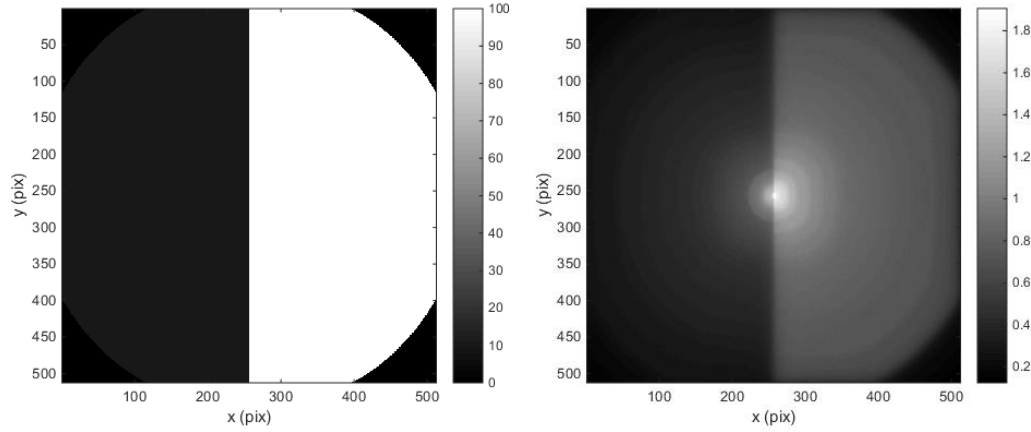


Figure 1. (Left) Nominal signal (stray-light free) for an illumination of an instrument with an extended scene with half the FOV illuminated at L_{max} and the other half at $L_{ref}=L_{max}/10$. (Right) Associated stray-light coming from ghosts for the 3MI instrument at 405 nm (ray-tracing simulations). The dark corners come from vignetting as the field of view of the instrument is smaller than the detector.

2. STRAY-LIGHT CORRECTION METHOD

Spatial Point Source Transmittance (SPST) maps are at the core of the stray-light correction method. By definition a SPST map is the stray-light profile at the detector when the instrument is illuminated with a punctual field. Moreover, the SPST map is normalized to a nominal signal equal to 1. If the SPST map associated to the field of view of each pixel of the instrument, it is possible to build matrix A_{SL} with the different SPST maps arranged as vectors. Then, if the nominal signal I_S is also rearranged as a vector, the modulation of matrix A_{SL} by the nominal signal gives the stray-light profile I_{SL} (equation 2). Indeed, the stray-light at the detector is the sum of the stray-light coming from each field, modulated by the signal in each of these fields. The measured signal consists of the sum of the nominal signal with the stray-light pattern (equation 3).

$$I_{SL} = A_{SL} \cdot I_S \quad (2)$$

$$I_S = I_0 + I_{SL} \quad (3)$$

$$\begin{pmatrix} I_{Mes}(1,1) \\ \dots \\ I_{Mes}(1,j) \\ \dots \\ I_{Mes}(1,N) \\ \dots \\ I_{Mes}(N,1) \\ \dots \\ I_{Mes}(N,j) \\ \dots \\ I_{Mes}(N,N) \end{pmatrix} = \begin{pmatrix} I_S(1,1) \\ \dots \\ I_S(1,j) \\ \dots \\ I_S(1,N) \\ \dots \\ I_S(N,1) \\ \dots \\ I_S(N,j) \\ \dots \\ I_S(N,N) \end{pmatrix} + \begin{pmatrix} SPST_{1,1}(1,1) & \dots & SPST_{i,j}(1,1) & \dots & SPST_{N,N}(1,1) \\ \dots & \dots & \dots & \dots & \dots \\ SPST_{1,1}(1,j) & \dots & SPST_{i,j}(1,j) & \dots & SPST_{N,N}(1,j) \\ \dots & \dots & \dots & \dots & \dots \\ SPST_{1,1}(1,N) & \dots & SPST_{i,j}(1,N) & \dots & SPST_{N,N}(1,N) \\ \dots & \dots & \dots & \dots & \dots \\ SPST_{1,1}(N,1) & \dots & SPST_{i,j}(N,1) & \dots & SPST_{N,N}(N,1) \\ \dots & \dots & \dots & \dots & \dots \\ SPST_{1,1}(N,j) & \dots & SPST_{i,j}(N,j) & \dots & SPST_{N,N}(N,j) \\ \dots & \dots & \dots & \dots & \dots \\ SPST_{1,1}(N,N) & \dots & SPST_{i,j}(N,N) & \dots & SPST_{N,N}(N,N) \end{pmatrix} \cdot \begin{pmatrix} I_S(1,1) \\ \dots \\ I_S(1,j) \\ \dots \\ I_S(1,N) \\ \dots \\ I_S(N,1) \\ \dots \\ I_S(N,j) \\ \dots \\ I_S(N,N) \end{pmatrix}$$

If we were able to estimate the stray-light associated to a given measured scene, $I_{SL\ est}$, we would be able to correct it from stray-light by subtracting it from the measured signal (equation 4). However, it is not possible to estimate the stray-light with equation 2 as it requires to modulate A_{SL} by I_S while I_S is precisely what we intend to find ultimately. Consequently, another way to estimate the stray-light must be found.

$$I_{corr} = I_{mes} - I_{SL\ est} \quad (4)$$

The idea of the stray-light correction is to estimate the stray-light by modulated the A_{SL} matrix by the measured signal. Indeed, if the stray-light is low enough compared to the nominal signal, this will provide a first estimation of the stray-light profile. A more accurate estimation of the stray-light can then be obtained by modulating A_{SL} by the estimated correction signal. This process is repeated iteratively with the set of equations (5) to (6) to converge toward the stray-light profile with an error below the performance requirement.

$$I_{Corr,0} = I_{mes} \quad (5)$$

$$I_{SL,k} = A_{SL} \cdot I_{Corr,k-1} \quad (6)$$

$$I_{Corr,k} = I_{mes} - I_{SL,k} \quad (7)$$

It can be shown analytically that the error dSL_k on the estimated stray-light for iteration k is given by equation (9). The behavior of dSL_k follows a damped harmonic oscillator-like behavior. Indeed, at iteration 1, the matrix A_{SL} is modulated by a scene which is over evaluated, giving an over evaluated stray-light pattern. However, at the next iteration the matrix is modulated by a scene which has been corrected by an over estimated stray-light, which gives an under estimated stray-light. With k increasing the error then converges toward zero.

$$I_{SL,k} = I_{SL} + dSL_k \quad (8)$$

$$dSL_k = \zeta_k \cdot A_{SL}^{k+1} \cdot I_{nom} \quad (9)$$

$$\text{with } \zeta_k = \begin{cases} 1 & \text{if } k \text{ odd} \\ -1 & \text{if } k \text{ even or } 0 \end{cases} \quad (10)$$

By developing the equations (8) to (10) with the assumption that $A_{SL} = \langle A_{SL} \rangle$, it can be shown that the mean of the error follows a sequence in power law given by equation (11), where $N \times N$ is the number of pixels at the detector. From this equation, it can be deduced that the absolute stray-light estimation error at iteration 1 depends quadratically on the stray-light level and linearly on the nominal signal. Moreover, this equation can be written as an exponential decay, hence emphasizing a decay rate which evolves as the logarithm of the stray-light level. Moreover, from equation (11) it is deduced that the stray-light algorithm converges only under the condition of equation (12), which basically requires that the integrated signal of a SPST map associated to any given field be below the associated nominal signal.

$$|dSL_k| = (\langle A_{SL} \rangle \cdot N^2)^{k+1} \cdot \langle I_{nom} \rangle \quad (11)$$

$$\langle A_{SL} \rangle \cdot N^2 < 1 \quad (12)$$

Equation (11) can be used to determine the number of iterations required to reach a given performance requirement. In the case of ghost stray-light in 3MI, we can deduce the quantitative value of equation (13) and insert it in equation (11). We then get equation (14) which shows the stray-light level at iteration 1. This value is already smaller than the performance requirement, however one more iteration is preferred to decrease the convergence error impact in the total error budget.

$$\langle A_{SL} \rangle \cdot N^2 = \frac{1}{94} \quad (13)$$

$$\langle dSL_1 \rangle = (\langle A_{SL} \rangle \cdot N^2)^2 \cdot \langle I_{nom} \rangle = 1.13 \cdot 10^{-4} \cdot \langle I_{nom} \rangle \quad (14)$$

3. MATRIX BINNING

Even for instruments with detector arrays with reasonable number of pixels, the matrix A_{SL} matrix filled with high resolution SPST maps is very large. With $N=512$ for the VNIR detector of 3MI, this makes about 68 billion elements in the A_{SL} matrix, leading to numerical issues. Hence, it is useful to reduce the size of A_{SL} by either reducing the resolution of the SPST maps or reducing the number of fields which are considered. For the latter, if less SPST maps are to be

considered, the best is to average SPST maps associated to neighboring fields, referred as field binning. The correction algorithm can be applied with both spatially and field binned data, though at the cost of errors in the stray-light correction process. It is thus necessary to set the binning parameters at a value which reduces sufficiently the size of matrix A_{SL} while not inducing errors up to the point where the correction error exceeds the correction performance requirement.

Figure 4 shows an example of how the error on the estimated stray-light evolves when varying the spatial binning dimension m , up to full resolution ($N=512$). The blue curve shows the error on an extended scene evaluated at 2 sigma percentile while the red curve is evaluated at 3 sigma percentile. The spatial binning should be selected such that the curve is below the requirement. However, margin should be taken as the requirement should be fulfilled considering the full error budget. In the particular case shown here it shows that a binning even on 2 by 2 pixels, giving a spatial dimension of 256 by 256 pixels, gives an error of half the requirement. This is a value too large for the error budget and no spatial binning is thus considered in this particular case. Such curves should however be done considering different type of scenes as they depend on the nominal signal. For example, if the extended scene has a transition at the center or close to an edge, it will change the total nominal signal and associated stray-light as well as the error on its estimation.

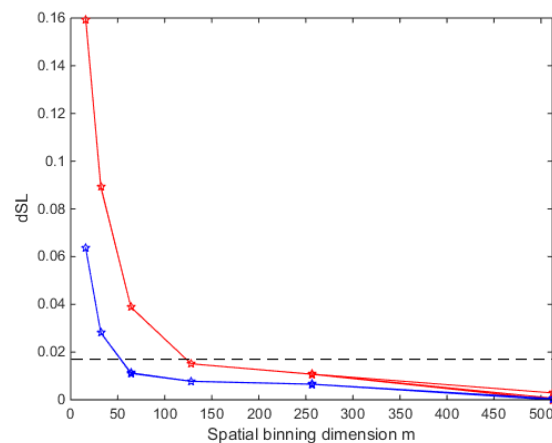


Figure 4. Example of curve which shows the error on the stray-light (2 sigma percentile in blue, 3 sigma percentile in red) as a function of the spatial binning.

In the case of field binning, the SPST maps are averaged for adjacent fields. However, the nominal signal which modulates the A_{SL} matrix is thus also binned. The effect of field binning actually applies only on this nominal signal modulation. If the field binning has no effect on the nominal signal, then whatever the field dependence of the SPST maps it will bring no error on the stray-light estimation. The effect of field binning must thus be evaluated for different profiles of the nominal scene. For example, in the case of an extended scene if the transition falls at the interface between two binned pixels of the nominal scene, the field binning will have no consequence. Hence, the error should be evaluated when the transition is inside a binned pixel. Then, curves similar as the one of Figure 4 can be extracted to estimate what the field binning dimension should be. It was shown that to fulfill our requirement the field binning in the case of 3MI was not smaller than 256×256 . Finally, for 3MI the correction algorithm is applied on a 512×512 spatial grid and 256×256 field grid.

4. SPST MAPS INTERPOLATION

In practice, the SPST maps associated to the field of each pixel of the detector is not available. Indeed, the calibration of an SPST map is a time consuming process and calibrating the full grid is not realistic (more than 200 000 fields in 3MI). An interpolation method was thus developed to increase artificially the number of maps available. The idea is to calibrate the SPST maps on a grid smaller than the full array and deduce the intermediate maps numerically.

The first method which was investigated is field domain interpolation. The principle is to convert SPST maps into Field Point Source Transmittance maps (FPST), which correspond to the stray-light on a given pixel of the detector as a function of the field of view (equation (15)). From there, a simple 2D interpolation, for example with polynomial kernel, is used to derive the stray-light on every pixel for intermediary fields. Figure 5 shows an example of FPST map interpolation. The drawback of this method is that features rapidly varying with the field cannot be correctly interpolated.

Hence, field domain interpolation provides poor accuracy on the stray-light interpolation and large errors when used in the stray-light correction algorithm.

$$SPST_{i,j}(k,l) = FPST_{k,l}(i,j) \tag{15}$$

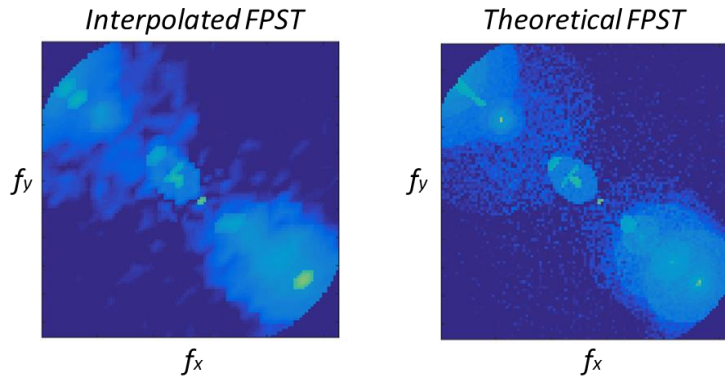


Figure 5. Field domain interpolation

Other methods which have been investigated are done by applying transformation of SPSTs in the spatial domain. Optical flux interpolation was an option but gave poor result. Thus, the proposed approach consisted in interpolating the SPST maps in the spatial domain based on an assumption of local symmetry. The principle is that if we want to get the SPST map associated to a given field which has not been calibrated, we should take the SPST map associated to the closest field which has been calibrated and operate a transformation (figure 6). As per the symmetry assumption, the closest SPST map is scaled by the ratio of the distances from the fields with respect to the center of the field of view (equation 16). Also, a rotation is applied to the SPST map with an angle given by equation 17.

$$s = \frac{|r_i|}{|r_c|} \tag{16}$$

$$\alpha = \cos^{-1}(\langle r_i | r_c \rangle) \tag{17}$$

The limitation of this method is that when the scale factor is smaller than one, or simply when rotating the SPST map, the interpolated map will present vignetted areas on the edges (Figure 7-middle). Hence, the interpolation is performed based on multiple neighbors: each time the edge is vignetted the next neighbor is used to fill the gap (figure 7-right). Moreover, another limitation of this method is that the scaling and rotation transformation starts to be non-physical when considering fields very close to the center of the field. Indeed, at these fields the scaling factor might be very large. For that reason, the calibration of SPST map is done on a denser grid close to the center of the field and in that area the closest neighbor is simply selected with no transformation.

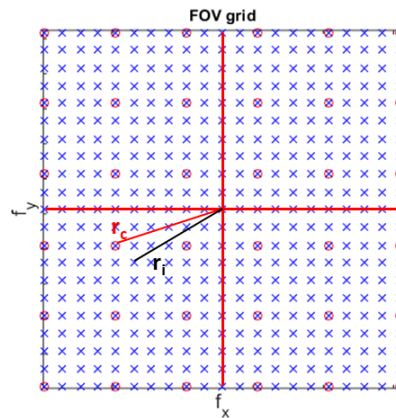


Figure 6. SPST map interpolation based on assumption of local symmetry

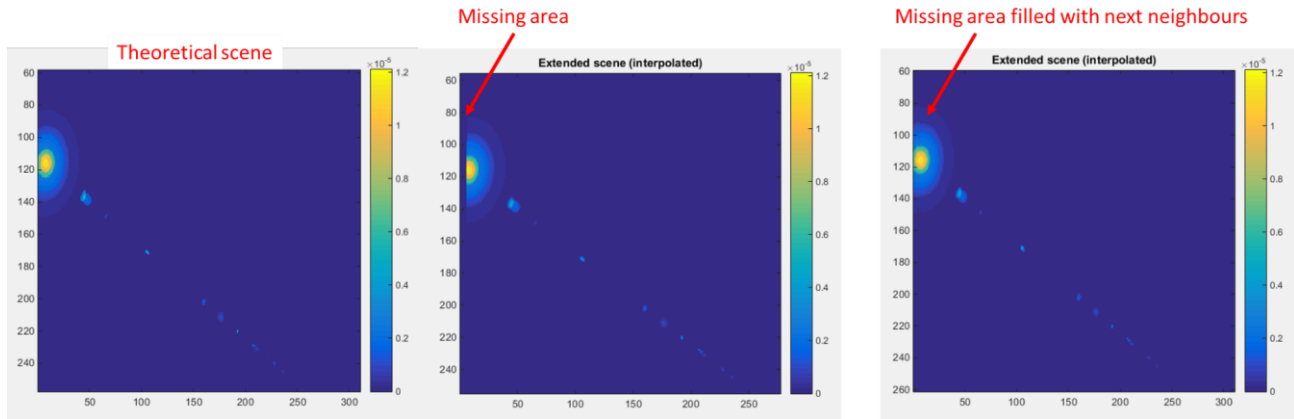


Figure 7. Interpolation of SPST map in the spatial domain based on local symmetry assumption. (Left) Theoretical SPST map. (Middle) SPST map interpolated based on one first neighbor. (Right) SPST map interpolated based on multiple neighbors.

5. CONCLUSIONS

Stray-light is a significant issue for space optical instruments. An algorithm has been developed to reduce the stray-light in the 3MI instrument by two orders of magnitude. The method consists in evaluating iteratively the estimated stray-light associated to any given scene and to subtract it to get the corrected signal. Binning of the SPST maps is required to reduce the amount of data which is stored and hence avoid numerical issues. It was however shown that, to fulfill the performance requirement, field binning should be done on a grid not smaller than 256×256 while spatially high resolution should be kept. In practice not all SPST maps are calibrated, an interpolation algorithm was thus develop to deduce the SPST map associated to any field. The field binning was then applied to these interpolated maps. With these conditions, Table 1 below gives the stray-light correction performance and shows that a residual stray-light by two orders of magnitude is achieved.

Table 1. Residual error on the estimated stray-light with interpolated SPST maps, considering an extended scene with transition between L_{max} and L_{ref} at different positions on the detector.

Transition position	Residual stray-light	
	1 sigma	2 sigma
x=385 pix	0.024 % · L_{ref}	0.060% · L_{ref}
x=256 pix	0.061 % · L_{ref}	0.148 % · L_{ref}
x=128 pix	0.080 % · L_{ref}	0.176 % · L_{ref}

REFERENCES

- [1] Fest, E., "Stray Light Analysis and Control", SPIE press, March 2013
- [2] Lionel Clermont, Céline Michel, Emmanuel Mazy, Charlotte Pachot, Niccolo Daddi, Carmine Mastrandread, Yvan G. Stockman, "Stray-light calibration and correction for the MetOp-SG 3MI mission", Proceedings of SPIE Vol. 10704, 1070406 (2018)
- [3] Bruno, U., Mastrandrea, C., Mosciarello, P., Gabrieli, R., Boldrini, F., Porciani, M., Langevin, M-N., "3MI: multi-viewing, multi-channel, multi-polarization imaging for METOp second generation", Proc. International Astronautical Congress, IAC-17-B1.3 (25-29 September 2017)